Metrological power of single-qubit dynamical Casimir effect in circuit QED

A.P. Costa^a, H.R. Schelb^a, A.V. Dodonov^{a,b,*}

^aInstituto de Física, Universidade de Brasília, Caixa Postal 04455, CEP 70910-900, Brasília, DF, Brasil ^bInternational Center of Physics, Institute of Physics, University of Brasilia, 70910-900, Brasilia, DF, Brazil

Abstract

We consider a nonstationary circuit QED system described by the quantum Rabi model, in which an artificial two-level atom with a tunable transition frequency is coupled to a single-mode resonator. We focus on regimes where the external modulation takes the form $\sin[\eta(t)t]$, with the modulation frequency $\eta(t)$ varying slowly and linearly in time near 2v and 4v, v being the resonator frequency. Starting from the vacuum state, we numerically compute the Quantum Fisher Information for single-mode phase and displacement estimation, showing that it significantly exceeds the classical limits for the same average photon number, even in the presence of dissipation. Thus, appropriate parametric modulation of the qubit not only simulates the dynamical Casimir effect but also enables the generation of nonclassical states of light that offer a metrological advantage over classical states of equivalent

Keywords: Quantum Rabi model, Quantum Metrology, Quantum Fisher Information, Dynamical Casimir effect, Metrological

We consider a nonstationary circuit QED system described by the a tunable transition frequency is coupled to a single-mode resorthe form sin[\(\eta(t)t)\)], with the modulation frequency \(\eta(t)\) varying frequency. Starting from the vacuum state, we numerically condisplacement estimation, showing that it significantly exceeds the presence of dissipation. Thus, appropriate parametric module but also enables the generation of nonclassical states of light that energy.

Reywords: Quantum Rabi model, Quantum Metrology, Quantum power**

1. Introduction

The most fundamental problem in metrology is the estimation of an unknown physical parameter, such as the amplitude of a DC or AC electromagnetic field, a small mechanical force, tiny displacements, coupling constants, etc [1, 2, 3, 4, 5, 6, 7, 8, 9, 10, 11]. Quantum metrology exploits quantum mechanical principles to enhance the precision of parameter estimation beyond classical limits (see reviews [12, 13, 14, 15] and references therein). It plays a crucial role in improving time and frequency standards, detecting gravitational waves, performing sensitive optical phase measurements, synchronizing clocks, conducting interferometry with interacting systems, magnetometry, and other applications [1, 2, 3, 14, 15, 16]. Measurement devices that use quantum systems in nonclassical states as "probes" can outperform their classical counterparts without consuming additional resources, where resources typically refer to the number of photons or atoms [14].

At the core of quantum metrology lies the concept of Quantum Fisher Information (QFI), a fundamental quantity that sets the ultimate sensitivity limit of any unbiased estimator through the quantum Cramér–Rao inequality [12, 13, 14]. The quantum Cramér–Rao inequality [12, 13, 14].

the ultimate sensitivity limit of any unbiased estimator through the quantum Cramér-Rao inequality [12, 13, 14]. The quantum Cramér-Rao bound depends solely on the density operator of the probe and the unknown parameter to be estimated, and it can, in principle, always be saturated by an appropriate measurement. Metrological power refers to any quantum enhancement arising from the nonclassicality of the probe state [4, 14], and QFI has become an essential tool for characterizing quantum states in terms of their sensitivity to external perturbations, thereby quantifying their metrological utility under

both ideal and noisy conditions. In particular, Gaussian states of the electromagnetic field have found numerous applications in quantum metrology [17, 18, 19, 16, 20], with the squeezed vacuum state playing a prominent role as the most sensitive pure Gaussian state for phase estimation (for a fixed average photon number) [21]. Furthermore, it has recently been shown that the QFI for quadrature-displacement sensing uniquely determines the maximum achievable precision enhancement in both local and distributed quantum metrology using any linear or nonlinear single-mode unitary transformation, providing a unified measure of metrological power [4].

In this Letter, we numerically study the QFI for non-Gaussian mixed states of the electromagnetic field generated from vacuum in a nonstationary circuit Quantum Electrodynamics (circuit QED) setup through parametric modulation of the qubit transition frequency. Circuit QED is one of the most promising platforms for quantum technologies, including quantum computing and quantum simulation, due to its high level of controllability and scalability. In circuit QED, superconducting qubits and resonators can be manipulated with unprecedented precision, while dissipative losses remain much smaller than the atom–field coupling strengths [22, 23, 24, 25, 26, 27, 28, 29, 30]. Notably, real-time control over the effective resonator frequency via an external magnetic field has enabled experimental implementations of analogs of the dynamical Casimir effect (DCE) [31, 32], i.e., the generation of photons from vacuum due to external variations of boundary conditions or material properties of the intracavity medium [33, 34]. The nonclassical properties of field states generated in circuit DCE were studied in [35, 36], while applications of thermal two-mode squeezed states for quantum metrology were analyzed in [37].

The controllability of qubit parameters also allows DCE

August 15, 2025 Preprint submitted to Elsevier

^{*}Corresponding author. Tel.: +55 61 31076076; Fax: +55 61 31077712 Email address: adodonov@unb.br (A.V. Dodonov)

analogs using a single qubit as the source of system perturbation [38, 39, 40, 41]. Here, we consider sinusoidal modulation of the qubit's level splitting with a linearly time-varying modulation frequency, as originally proposed in [42]. We focus on modulation frequencies near 2ν and 4ν , where ν is the resonator frequency, leading to photon creation from vacuum via two- and four-photon transitions, respectively [43]. We model the system using the standard Markovian master equation of Quantum Optics with a time-dependent Rabi Hamiltonian and numerically study the evolution of the QFI for phase [21, 17] and phasespace displacement [6, 44] estimations, as well as the average photon number, its variance, qubit excitation, resonator field purity, and negativity. Our main finding is that, for appropriately chosen system parameters, one can generate mixed states of light with high QFI values unattainable by classical field states with the same energy. Moreover, in some cases, these field states exhibit higher QFI values than the squeezed vacuum state for the same average photon number. To our knowledge, this is the first demonstration that single-qubit DCE can be used to produce nonclassical states of light with applications in quantum metrology.

2. Mathematical formalism

We consider a two-level artificial atom (qubit) in a superconducting resonator of frequency ν . The system is described by the quantum Rabi Hamiltonian [45, 46, 47, 48] (\hbar = 1)

$$H = \frac{\Omega(t)}{2}\sigma_z + \nu n + g\left(a + a^{\dagger}\right)(\sigma_+ + \sigma_-) , \qquad (1)$$

where a and a^{\dagger} are the annihilation and creation operators of the electromagnetic field, $n=a^{\dagger}a$ is the photon number operator and g is the light–matter coupling constant [49, 50, 51]. The atomic operators are $\sigma_z=|e\rangle\langle e|-|g\rangle\langle g|,\,\sigma_+=|e\rangle\langle g|$ and $\sigma_-=\sigma_+^{\dagger}=|g\rangle\langle e|,$ where $|g\rangle$ and $|e\rangle$ denote the ground and the excited states, respectively. To induce the photon generation from vacuum, we suppose that the atomic transition frequency is modulated externally as

$$\Omega(t) = \Omega_0 + \varepsilon \sin[\eta(t)t], \qquad (2)$$

where Ω_0 is the bare qubit frequency, $\varepsilon \ll \Omega_0$ is the modulation amplitude and $\eta(t)$ is the time-dependent modulation frequency. Following the proposal [42], we consider a slow linear sweep, $\eta(t) = \eta_0 + \alpha t$, where η_0 and α are constant parameters. We take into account the effects of weak Markovian dissipation [27, 52] via the the standard master equation of Quantum Optics, also known as Gorini-Kossakowski-Sudarshan-Lindblad (GKSL) master equation,

$$\frac{\partial \rho}{\partial t} = -i \left[H, \rho \right] + \gamma \mathcal{D}[\sigma_{-}] \rho + \gamma_{\phi} \mathcal{D}[\sigma_{z}] \rho + \kappa \mathcal{D}[a] \rho, \quad (3)$$

where ρ is the total system density operator, $\gamma \left(\gamma_{\phi} \right)$ is the atomic damping (pure dephasing) rate, κ is the cavity damping rate, $\mathcal{D}[\sigma]\rho \equiv \sigma\rho\sigma^{\dagger} - \left(\sigma^{\dagger}\sigma\rho + \rho\sigma^{\dagger}\sigma\right)/2$ is the Lindblad superoperator and we assumed zero temperature reservoirs.

We now briefly review the concept of quantum Fisher information, whose properties are discussed in detail in the reviews [14, 12, 13, 15]. To estimate an unknown parameter θ , one collects measurement outcomes from experiments and constructs an estimator $\hat{\theta}$, a function of the data that provides the best guess for θ . Common examples of parameter estimation using bosonic fields include the estimation of phase and phase-space displacements. For an unbiased estimator, in the limit of a large number n of measurements, the precision is bounded from below by the Cramér–Rao bound: $\Delta^2 \theta \ge [nF(\theta)]^{-1}$. Here

$$F(\theta) = \int dx p(x|\theta) \left[\frac{\partial}{\partial \theta} \ln p(x|\theta) \right]^2 \tag{4}$$

is the Fisher information of the probability distribution $p(x|\theta)$, which is the conditional probability of obtaining measurement outcome x given the parameter value θ . Higher precision can be achieved by increasing the number of measurements and/or the Fisher information $F(\theta)$.

The QFI, $\mathcal{F}(\rho, \theta)$, is the supremum of the Fisher information over all possible quantum measurements described by positive operator-valued measures (POVMs) [14, 15, 13], where ρ denotes the density operator of the system used as the probe. In this sense, OFI quantifies the maximum information about θ that can be imprinted onto the probe state. The ultimate limit on extracting information about an unknown parameter θ via a quantum measurement is given by the quantum Cramér-Rao bound, $\Delta^2 \theta \ge [n\mathcal{F}(\rho, \theta)]^{-1}$, which depends only on the probe's density operator and the unknown parameter θ . Intuitively, for states that differ slightly in the value of θ , the more distinguishable the states, the more precisely θ can be estimated. Notably, QFI is independent of the final measurement procedure. Optimizing measurement precision thus involves choosing a probe state with large QFI and a measurement strategy such that Eq. (4) approaches the QFI. It can be shown [14] that the quantum Cramér-Rao bound can always be saturated by an appropriate measurement, so $\mathcal{F}(\rho,\theta)$ quantifies the usefulness of a probe ρ for measuring a given θ .

For the *phase estimation* using unitary encoding, the QFI reads [14]

$$\mathcal{F}_{ph} = \frac{1}{2} \sum_{i,j} \frac{\left(p_i - p_j\right)^2}{p_i + p_j} \left| \langle i | \hat{n} | j \rangle \right|^2 , \qquad (5)$$

where p_i and $|i\rangle$ are the eigenvalues and eigenvectors of the reduced cavity density operator, $\rho_{cav}(t) = \mathrm{Tr}_{qubit}[\rho(t)]$. The inequality $\mathcal{F}_{ph} \leq \langle n \rangle_{clas}$ holds for any classical state ρ_{clas} , where $\langle n \rangle_{clas} = \mathrm{Tr}(\rho_{clas}a^{\dagger}a)$ is the corresponding average photon number. Therefore, any quantum state with $\mathcal{F}_{ph} > \langle n \rangle$ exhibits metrological power [14, 15]. Among pure Gaussian states, the squeezed vacuum state, $\rho_{sv} = \exp\left[(\varepsilon^*a^2 - \varepsilon a^{\dagger 2})/2\right]|0\rangle$ with a complex parameter ε , is the most sensitive state for a given average photon number. Its QFI is $\mathcal{F}_{ph}(\rho_{sv}) = 2(\langle n \rangle_{sv}^2 + \langle n \rangle_{sv})$. So we also calculate numerically the ratio

$$r = \frac{1}{2} \frac{\mathcal{F}_{ph}}{\langle n \rangle^2 + \langle n \rangle} \,, \tag{6}$$

which compares the QFI of the field state generated via singlequbit DCE with that of the squeezed vacuum state generated in the standard DCE [33, 34], assuming the same average photon number.

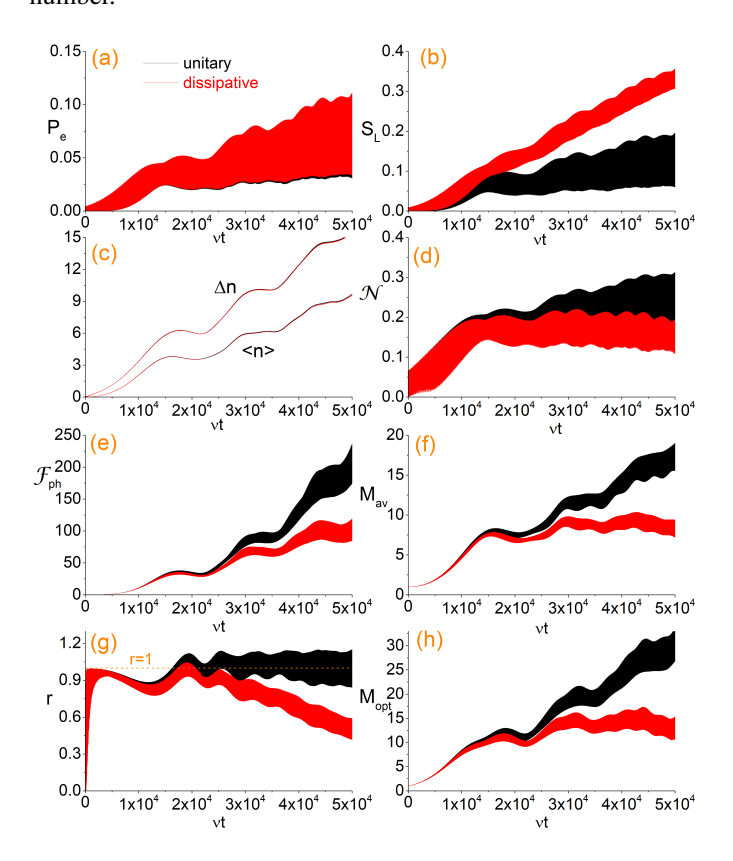


Figure 1: Behavior of some relevant quantities under unitary (black curves) and dissipative (red curves) dynamics, obtained by solving numerically the master equation (3) for the initial state $|g,0\rangle$ and the two-photon DCE regime. a) Atomic excitation probability (the difference between the unitary and dissipative evolutions is practically invisible). The curves appear broad due to fast oscillations (with frequencies ~ ν). b) Linear entropy of the cavity field, which measures entanglement under unitary evolution. c) Average photon number and the standard deviation. d) Negativity, Eq. (10); nonzero values attest entanglement. e) Quantum Fisher Information for single mode phase estimation, Eq. (5). f) M_{av} , Eq. (8). g) Ratio r, Eq. (6). h) M_{opt} , Eq. (9). Parameters: $g=0.05\nu$, $\Omega_0=0.5\nu$, $\varepsilon=0.08\Omega_0$, $\eta_0=2.00655\nu$, $\alpha=2\times10^{-8}\nu^2$ and $\lambda=\lambda_\phi=\kappa=10^{-6}\nu$.

To estimate the *phase-space displacement* of a single-mode field, one must study the 2×2 quantum Fisher information matrix [14] with the elements

$$\left(F_{disp}\right)_{kl} = \sum_{i,j} \frac{\left(p_i - p_j\right)^2}{p_i + p_j} \langle i | x^{(k)} | j \rangle \langle j | x^{(l)} | i \rangle , \qquad (7)$$

where $x^{(1)} = a + a^{\dagger}$ and $x^{(2)} = (a - a^{\dagger})/i$. The *average* Fisher information over all possible quadrature directions is

$$M_{av} = \frac{1}{4} \operatorname{Tr} \left(\mathbf{F}_{disp} \right) , \qquad (8)$$

while the *maximum* Fisher information over all possible quadrature directions reads

$$M_{opt} = \frac{1}{2} \lambda_{\text{max}} \left(\mathbf{F}_{disp} \right) , \qquad (9)$$

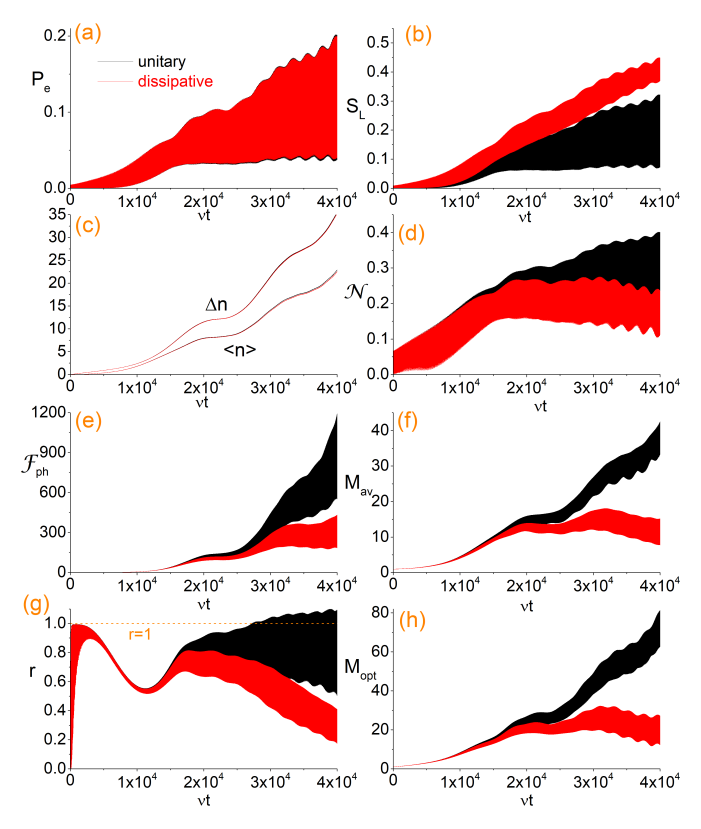


Figure 2: Similar to Fig. 1, but for slightly different modulation form: $\eta_0 = 2.00715 v$ and $\alpha = -5 \times 10^{-8} v^2$. Notice that $\langle n \rangle$ and QFI are much higher than in Fig. 1, illustrating how small changes in the modulation form strongly affect the system dynamics.

where $\lambda_{\max}(\mathbf{F}_{disp})$ is the maximum eigenvalue of \mathbf{F}_{disp} . For any classical state, the following inequalities hold: $M_{av}(\rho_{clas}), M_{opt}(\rho_{clas}) \leq 1$. Therefore, any quantum state with $M_{av}(\rho_{cav}) > 1$ or $M_{opt}(\rho_{cav}) > 1$ also offers metrological power for the displacement estimation.

3. Numeric results

We solved numerically the master equation (3) for the initial state $|g,0\rangle$, using the Runge-Kutta-Verner fifth-order and sixth-order method. Besides the metrological quantities described in the previous section (\mathcal{F}_{ph} , r, M_{av} and M_{opt}), we calculate the qubit excitation probability, $P_e = \text{Tr}\left[\rho|e\rangle\langle e|\right]$, the average photon number $\langle n\rangle$, its standard deviation, $\Delta n = \sqrt{\langle n^2\rangle - \langle n\rangle^2}$, the linear entropy of the cavity field, $S_L = 1 - \text{Tr}\left(\rho_{cav}^2\right)$, and the negativity [53]

$$\mathcal{N}(\rho) = \left| \sum_{i < 0} \lambda_i \right| \,, \tag{10}$$

where λ_i are the eigenvalues of the partial transpose of ρ with respect to any subsystem. For any bipartite system, nonzero negativity implies entanglement. In all the figures presented below, we consider the modulation amplitude $\varepsilon = 0.08\Omega_0$ and the realistic dissipative parameters $\lambda = \lambda_\phi = \kappa = 10^{-6} v$ [54]. For

comparison, the system behavior under the unitary dynamics is also shown; in this case, the linear entropy, beside measuring the purity of the cavity field, also attests entanglement.

In Figs. 1 and 2, we set $g=0.05\nu$ (below the ultrastrong regime [49, 50]), $\Omega_0=0.5\nu$ and consider a linear sweep of the modulation frequency in the vicinity of the standard DCE resonance, $\eta\approx 2\nu$. In Fig. 1, we assume $\eta_0=2.00655\nu$ and $\alpha=2\times 10^{-8}\nu^2$, while in Fig. 2, $\eta_0=2.00715\nu$ and $\alpha=-5\times 10^{-8}\nu^2$. In both cases, we see that a few dozen of photons are generated from vacuum, while the qubit excitation probability remains relatively low for the considered time interval, $P_e\lesssim 0.2$. As expected, the cavity field becomes entangled with the qubit (as attested by nonzero negativity), and its linear entropy increases with time. For example, for times $\nu t\lesssim 3\times 10^4$, the purities of the field states are $1-S_L\gtrsim 0.7$.

The main results of this work, within the context of quantum metrology, are shown in panels e-h of Figs. 1-4. In the panels 1e and 2e, we see that the QFI for phase estimation exceeds significantly the average photon number, attesting that the generated (mixed) cavity field states indeed present metrological power. While for the considered dissipative rates the dynamics of P_e , $\langle n \rangle$ and Δn are practically unaffected by the dissipation, this is not true for the linear entropy, negativity and QFI, emphasizing the importance of taking the losses into account. Nonetheless, the metrological power persists even in the presence of dissipation. From the panels 1g and 2g, we see that the ratio r can reach values greater than 1, without dissipation, or of the order of 0.6 with dissipation, meaning that the produced mixed cavity field states possess metrological power comparable to that of the squeezed vacuum states. In panels f-h of Figs. 1 and 2 we also see that M_{av} and M_{opt} are significantly larger than 1, attaining values as large as $M_{av} \approx 40$ (without dissipation) and $M_{av} \approx 20$ (with dissipation).

To better understand the origin of the metrological power in our case, panels 3a and 3b show the photon number distribution (in logarithmic scale) of the field states at the time instants $vt = 2 \times 10^4$ and $vt = 3 \times 10^4$, for the parameters used in Figs. 1 and 2. These times were chosen arbitrarily to present relatively high values of r and M_{av} , while keeping the discrepancies between the unitary and dissipative dynamics reasonably small. We observe that the distributions are quite broad and not monotonically decreasing, so the large variance of the photon number partially explains the high values of the QFI. However, the variance alone does not determine the QFI for the considered mixed states, since the QFI is strongly affected by dissipation, whereas the standard deviation is not.

Finally, in Figs. 4 and 5, we consider the 4-photon DCE regime [43], $\eta \approx 4\nu$, near the three-photon resonance of the Rabi Hamiltonian [55, 56]. We set $g=0.15\nu$ (in the ultrastrong coupling regime), $\Omega_0=2.9\nu$, $\eta_0=3.931\nu$, and consider $\alpha=8\times10^{-7}\nu^2$ (Fig. 3) and $\alpha=2\times10^{-6}\nu^2$ (Fig. 4). In this regime, the qubit displays a higher probability of excitation, $P_e\gtrsim0.5$ for certain time intervals, and the purity of the cavity field state may drop below 0.5 due to significant qubit–field entanglement. The QFI is significantly larger than the average photon number, while the ratio r can exceed 1 (see Fig. 5g), indicating that the generated states may possess more metro-

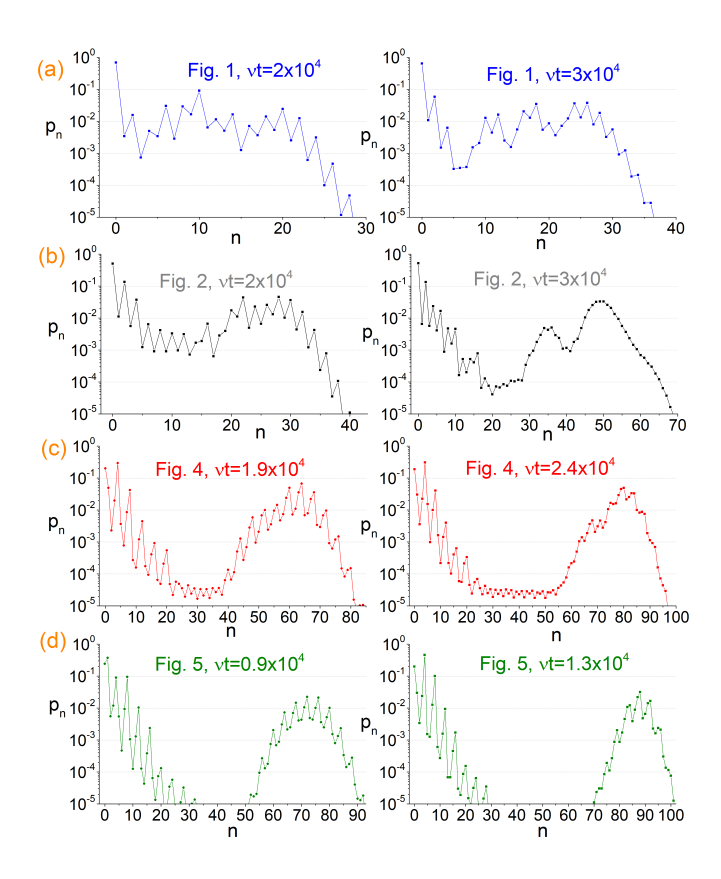


Figure 3: Photon number distribution (in the log-scale) for the time instants indicated in the plots. For the parameters of: a) Fig. 1; b) Fig. 2; c) Fig. 4. d) Fig. 5.

logical power than squeezed vacuum states with the same average photon number. For the considered time interval, M_{av} and M_{opt} also reach high values, on the order of $M_{av} \approx 60$ (without dissipation) and $M_{av} \approx 30$ (with dissipation). Panels 3c and 3d show the photon number distribution of the cavity field states at selected time instants. We observe that the photon number distribution exhibits local peaks when n/4 is an integer, has a large variance, and resembles a bimodal distribution for the times considered. Note that an analytical description of our system in the considered parameter regimes is challenging, since nearly 100 Fock states actively participate in the dynamics, and the counter-rotating terms in the Rabi Hamiltonian cannot be neglected.

4. Conclusions

In conclusion, we numerically studied a dissipative circuit QED system in which the qubit level splitting undergoes sinusoidal external modulation with a linearly varying frequency. We considered regimes where the qubit is far detuned from the resonator and the modulation frequencies are close to the resonances corresponding to the two- and four-photon dynamical Casimir effects. We showed that, for carefully chosen parameters, it is possible to generate nonclassical states of light from the vacuum with high quantum Fisher information for phase and displacement estimation, capable of outperforming

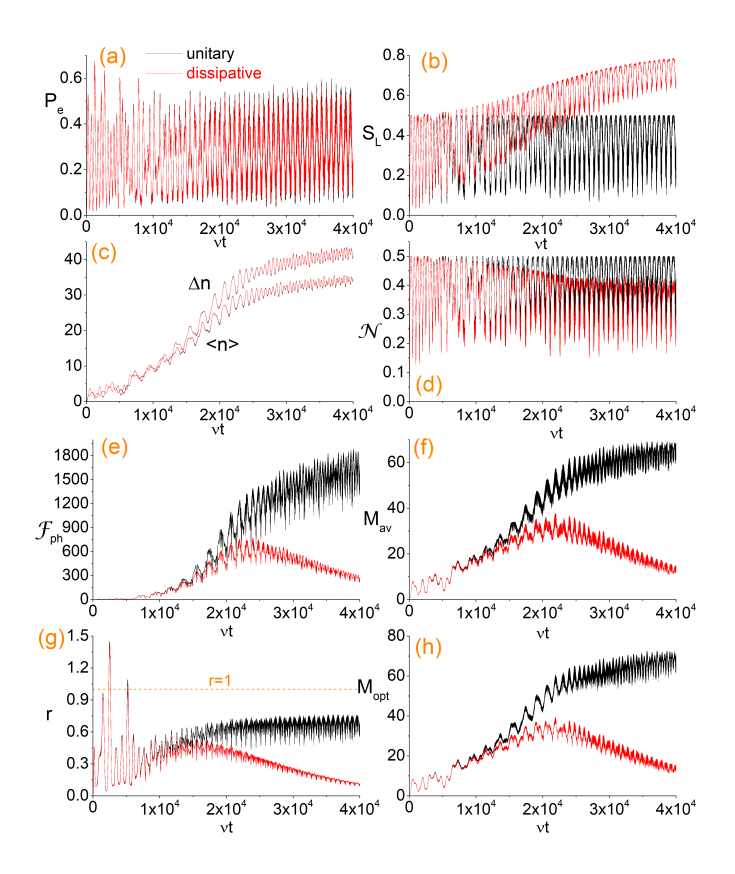


Figure 4: Similar to Fig. 1, but for the 4-photon DCE with parameters: $g=0.15\nu$, $\Omega_0=2.9\nu$ and $\eta_0=3.931\nu$, $\alpha=8\times10^{-7}\nu^2$.

squeezed vacuum states with the same average photon number. The states generated in our scheme are intrinsically mixed and exhibit photon number distributions that are markedly different from those of standard squeezed states. Therefore, single-qubit DCE, in addition to enabling the creation of excitations from the vacuum, may also serve as a resource for producing states of light with significant metrological power.

5. Acknowledgment

A. P. C. acknowledges the financial support by the Brazilian agency Coordenação de Aperfeiçoamento de Pessoal de Nível Superior (CAPES, Finance Code 001). H. R. S. acknowledges the financial support of the Brazilian agency Fundação de Apoio à Pesquisa do Distrito Federal (FAPDF, program PIBIC). A. V. D. acknowledges a partial financial support of the Brazilian agency Fundação de Apoio à Pesquisa do Distrito Federal (FAPDF, grant number 00193-00001817/2023-43).

References

- T. Nagata, R. Okamoto, J.L. O'Brien, K. Sasaki, and S. Takeuchi, Beating the standard quantum limit with four entangled photons, Science 316 (2007) 726.
- [2] W. Muessel, H. Strobel, D. Linnemann, D. B. Hume, and M.K. Oberthaler, Scalable Spin Squeezing for Quantum Enhanced Magnetometry with Bose-Einstein Condensates, Phys. Rev. Lett. 113 (2014) 103004.

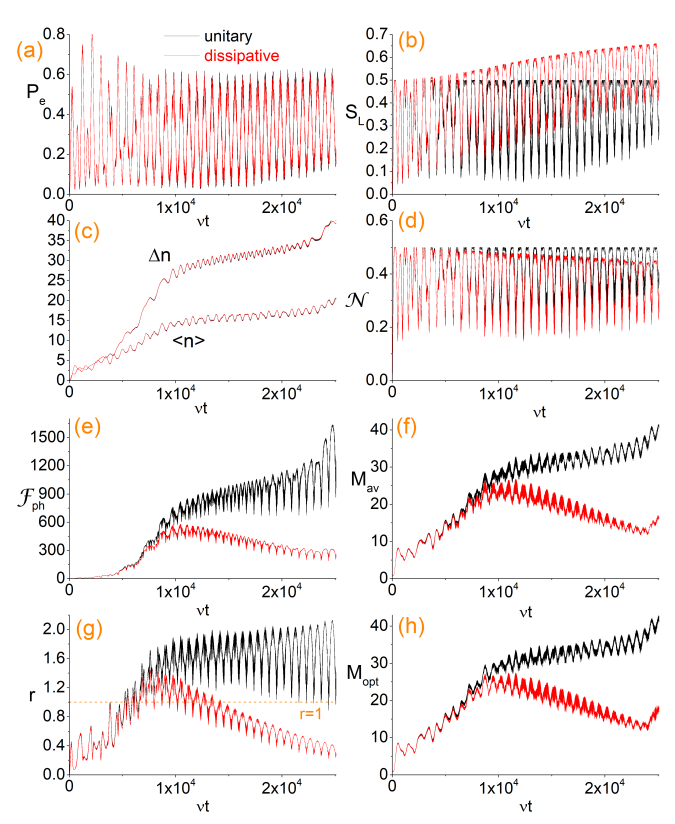


Figure 5: Similar to Fig. 4, but for the parameter $\alpha = 2 \times 10^{-6} v^2$.

- [3] The LIGO Scientific Collaboration, A gravitational wave observatory operating beyond the quantum shot-noise limit, Nat. Phys. 7 (2011) 962.
- [4] W. Ge, K. Jacobs and M.S. Zubairy, The power of microscopic nonclassical states to amplify the precision of macroscopic optical metrology, npj Quant. Inf. 9 (2023) 5.
- [5] V. Giovannetti, S. Lloyd and L. Maccone, Advances in quantum metrology, Nat. Photon. 5 (2011) 222.
- [6] M. Penasa, S. Gerlich, T. Rybarczyk, V. Métillon, M. Brune, J.M. Raimond, S. Haroche, L. Davidovich, and I. Dotsenko, Measurement of a microwave field amplitude beyond the standard quantum limit, Phys. Rev. A 94 (2016) 022313.
- [7] C.L. Latune, B.M. Escher, R.L. de Matos Filho, and L. Davidovich, Quantum limit for the measurement of a classical force coupled to a noisy quantum-mechanical oscillator, Phys. Rev. A 88 (2013) 042112.
- [8] G.A. Smith, A. Silberfarb, I.H. Deutsch, and P. S. Jessen, Efficient quantum state estimation by continuous weak measurement and dynamical control, Phys. Rev. Lett. 97 (2006) 180403.
- [9] L. Zhang, A. Datta and I.A. Walmsley, Precision metrology using weak measurements. Phys. Rev. Lett. 114 (2015) 210801.
- [10] X.Y. Xu, Y. Kedem, K. Sun, L. Vaidman, C.F. Li, and G.C. Guo, Phase estimation with weak measurement using a white light source. Phys. Rev. Lett. 111 (2013) 033604.
- [11] B. Gong, Y. Yang and W. Cui, Quantum parameter estimation via dispersive measurement in circuit QED, Quant. Inf. Process. 17 (2018) 301.
- [12] D. Petz and C. Ghinea, Introduction to Quantum Fisher Information, Quantum Probability and Related Topics, 261-281 (2011). DOI: 10.1142/9789814338745_0015
- [13] G. Tóth and I. Apellaniz, Quantum metrology from a quantum information science perspective, J. Phys. A: Math. Theor. 47 (2014) 424006.
- [14] K.C. Tan and H. Jeong, Nonclassical Light and Metrological Power: An Introductory Review, AVS Quantum Sci. 1 (2019) 014701.
- [15] J.S. Sidhu and P. Kok, A Geometric Perspective on Quantum Parameter Estimation, AVS Quantum Sci. 2 (2020) 014701. DOI: https://doi.org/10.1116/1.5119961

- [16] Z. Jiang, Quantum Fisher information for states in exponential form, Phys. Rev. A 89 (2014) 032128.
- [17] M. Aspachs, J. Calsamiglia, R. Muñoz-Tapia, and E. Bagan, Phase estimation for thermal Gaussian states, Phys. Rev. A 79 (2009) 033834.
- [18] O. Pinel, P. Jian, N. Treps, C. Fabre, and D. Braun, Quantum parameter estimation using general single-mode Gaussian states, Phys. Rev. A 88 (2013) 040102(R).
- [19] M. Bina, F. Grasselli and M.G.A. Paris, Continuous-variable quantum probes for structured environments, Phys. Rev. A 97 (2018) 012125.
- [20] D. Šafránek, A.R. Lee and I. Fuentes, Quantum parameter estimation using multi-mode Gaussian states, New J. Phys 17 (2015) 073016.
- [21] A. Monras, Optimal phase measurements with pure Gaussian states, Phys. Rev. A 73 (2006) 033821.
- [22] A. Blais, A.L. Grimsmo, S.M. Girvin, and A. Wallraff, Circuit quantum electrodynamics, Rev. Mod. Phys. 93 (2021) 025005.
- [23] T.I. Andersen et al., Thermalization and criticality on an analogue–digital quantum simulator, Nature 638 (2025) 79.
- [24] Y. Zhang, S. Jahanbani, A. Riswadkar, S. Shankar, and A.C. Potter, Sequential quantum simulation of spin chains with a single circuit QED device, Phys. Rev. A 109 (2024) 022606.
- [25] Z.-Y. Wei, J.I. Cirac and D. Malz, Generation of photonic tensor network states with circuit QED, Phys. Rev. A 105 (2022) 022611.
- [26] A. Miessen, D.J. Egger, I. Tavernelli, and G. Mazzola, Benchmarking Digital Quantum Simulations Above Hundreds of Qubits Using Quantum Critical Dynamics, PRX Quant. 5 (2024) 040320.
- [27] A. Blais, A.L. Grimsmo, S.M. Girvin, A. Wallraff, Circuit quantum electrodynamics, Rev. Mod. Phys. 93 (2021) 025005.
- [28] J.Q. You and F. Nori, Atomic physics and quantum optics using superconducting circuits, Natur 474 (2011) 589.
- [29] G. Wendin, Quantum information processing with superconducting circuits: A review, Rep. Prog. Phys. 80 (2017) 106001.
- [30] X. Gu, A.F. Kockum, A. Miranowicz, Y.-x. Liu and F. Nori, Microwave photonics with superconducting quantum circuits, Phys. Rep. 718-719 (2017) 1.
- [31] C.M. Wilson, G. Johansson, A. Pourkabirian, M. Simoen, J.R. Johansson, T. Duty, F. Nori, and P. Delsing, Observation of the dynamical Casimir effect in a superconducting circuit, Nature 479 (2011) 376.
- [32] P. Lähteenmäki, G.S. Paraoanu, J. Hassel, and P.J. Hakonen, Dynamical Casimir effect in a Josephson metamaterial, Proc. Nat. Acad. Sci. USA 110 (2013) 4234.
- [33] P.D. Nation, J.R. Johansson, M.P. Blencowe, and F. Nori, Colloquium: Stimulating uncertainty: Amplifying the quantum vacuum with superconducting circuits, Rev. Mod. Phys. 84 (2012) 1.
- [34] V. Dodonov, Fifty Years of the Dynamical Casimir Effect, Physics 2 (2020) 67.
- [35] C. Sabín, I. Fuentes and G. Johansson, Quantum discord in the dynamical Casimir effect, Phys. Rev. A 92 (2015) 012314.
- [36] J.R. Johansson, G. Johansson, C.M. Wilson, O. Delsing, and F. Nori, Nonclassical microwave radiation from the dynamical Casimir effect, Phys. Rev. A 87 (2013) 043804.
- [37] A. Wilkins and C. Sabín, Quantum estimation via parametric amplification in circuit-QED arrays, Phys. Rev. A 92 (2015) 062102.
- [38] S. De Liberato, C. Ciuti and I. Carusotto, Quantum vacuum radiation spectra from a semiconductor microcavity with a time-modulated vacuum Rabi frequency, Phys. Rev. Lett. 98 (2007) 103602.
- [39] A. V. Dodonov, Photon creation from vacuum and interactions engineering in nonstationary circuit QED, J. Phys.: Conf. Ser. 161 (2009) 012029.
- [40] S. De Liberato, D. Gerace, I. Carusotto, and C. Ciuti, Extracavity quantum vacuum radiation from a single qubit, Phys. Rev. A 80 (2009) 053810.
- [41] A. V. Dodonov, Analytical description of nonstationary circuit QED in the dressed-states basis, J. Phys. A: Math. Theor. 47 (2014) 285303.
- [42] A.V. Dodonov, B. Militello, A. Napoli, and A. Messina, Effective Landau-Zener transitions in the circuit dynamical Casimir effect with timevarying modulation frequency, Phys. Rev. A 93 (2016) 052505.
- [43] A. V. Dodonov, Dynamical Casimir effect via four- and five-photon transitions using a strongly detuned atom, Phys. Rev. A 100 (2018) 032510.
- [44] A. Ritboon, L. Slodička and R. Filip, Sequential phonon measurements of atomic motion, Quantum Sci. Technol. 7 (2022) 015023.
- [45] J. Larson and Th.K. Mavrogordatos, The Jaynes-Cummings Model and Its Descendants (IOP Publishing, Bristol, 2021).

- $https://arxiv.org/abs/2202.00330\ (2024).$
- [46] D. Braak, Q.-H. Chen, M.T. Batchelor, and E. Solano, Semi-classical and quantum Rabi models: in celebration of 80 years, J. Phys. A: Math. and Theor. 49 (2016) 300301.
- [47] D. Braak, Integrability of the Rabi Model, Phys. Rev. Lett. 107 (2011) 100401
- [48] Q. Xie, H. Zhong, M.T. Batchelor, and C. Lee, The quantum Rabi model: solution and dynamics, J. Phys. A.: Math. Theor. 50 (2017) 113001.
- [49] A.F. Kockum, A. Miranowicz, S. De Liberato, S. Savasta, and F. Nori, Ultrastrong coupling between light and matter, Nat. Rev. Phys. 1 (2019) 19
- [50] P. Forn-Díaz, L. Lamata, E. Rico, J. Kono, and E. Solano, Ultrastrong coupling regimes of light-matter interaction, Rev. Mod. Phys. 91 (2019) 025005.
- [51] D.Z. Rossatto, C.J. Villas-Bôas, M. Sanz, and E. Solano, Spectral classification of coupling regimes in the quantum Rabi model, Phys. Rev. A 96 (2017) 013849.
- [52] D.S. Veloso and A.V. Dodonov, Prospects for observing dynamical and anti- dynamical Casimir effects in circuit QED due to fast modulation of qubit parameters, J. Phys. B: At. Mol. Opt. Phys. 48 (2015) 165503.
- [53] G. Vidal and R.F. Werner, Computable measure of entanglement, Phys. Rev. A 65 (2002) 032314.
- [54] O. Milul et al., Superconducting Cavity Qubit with Tens of Milliseconds Single-Photon Coherence Time, PRX Quant. 4 (2023) 030336.
- [55] K.K.W. Ma and C.K. Law, Three-photon resonance and adiabatic passage in the large-detuning Rabi model, Phys. Rev. A 92 (2015) 023842.
- [56] M.V.S. de Paula, M.A. Damasceno Faustino, A.V. Dodonov, Comparison of Quantum and Semiclassical Rabi models near multiphoton resonances in the presence of parametric modulation, arXiv:2507.08271.